CRYSTAL ORIENTATION, MOSAICITY AND STRAIN IN MOSAIC CRYSTALS STUDIED BY TIME-OF-FLIGHT NEUTRON TRANSMISSION

Javier Santisteban*, Mark Daymond**, Lyndon Edwards*

* Department of Materials Engineering, The Open University, Milton Keynes MK7 6AA, United Kingdom
** ISIS, Rutherford Appleton Laboratory, Chilton, Didcot, UK

ABSTRACT

We introduce the basic features of the neutron transmission by mosaic crystals through demonstration experiments comprising in-situ loading tests on plastically deformed Cu crystals, originally used as neutron monochromators. We show that these experiments can be used to monitor the variation in orientation, mosaic spread and interplanar distances, that occur as a result of elastic or plastic deformation. Distinctive features of this technique are the ability to study many crystal reflections simultaneously, together with the possibility of 2D spatial resolution. In its present state, it is possible to study the spatial distribution of a specimen's deformation in-situ over an area of 25x25 mm^2 with 2 mm spatial resolution. We report the anisotropic evolution of the mosaic spread of a crystal as a result of plastic deformation, and its dependence on the macroscopic shear strain and applied stress.

1. INTRODUCTION

Monocrystals are used in neutron spectrometers as monochromators to select specific neutron wavelengths. The monocrystals used as monochromators consist of slightly misaligned smaller blocks. The mosaic spread or *mosaicity* of the crystal is a measure of this misalignment. The diffracted intensity from a neutron monochromator is roughly proportional to its mosaicity. Monochromators are usually required to display an anisotropic mosaic spread, with the mosaicity in the diffraction plane matching the incident beam divergence, whilst normal to this plane the mosaicity is kept low for efficient focussing of the beam on the sample. However, crystals are grown rather perfectly, with mosaicities of a few minutes of arc, making them useless as neutron monochromators. So, several methods have been proposed to increase the mosaic

spread of perfect crystals through elastic bending or plastic deformation (Frey 1974). The production of mosaic crystals with a controlled an homogeneous mosaicity by plastic deformation is not an easy task, and so far the process is quite inefficient in both time and material: a large proportion of the crystals are unusable at the end of the production stage and a significant amount of time is spent in testing and characterization. Besides this, the plastic deformation of monocrystals is of great interest as these studies may reveal basic phenomena of deformation processes.

Here, we introduce a new experimental technique capable of monitoring the variation in orientation, mosaicity and interplanar distances in mosaic crystals; based on a spectroscopic analysis of the transmitted neutrons.

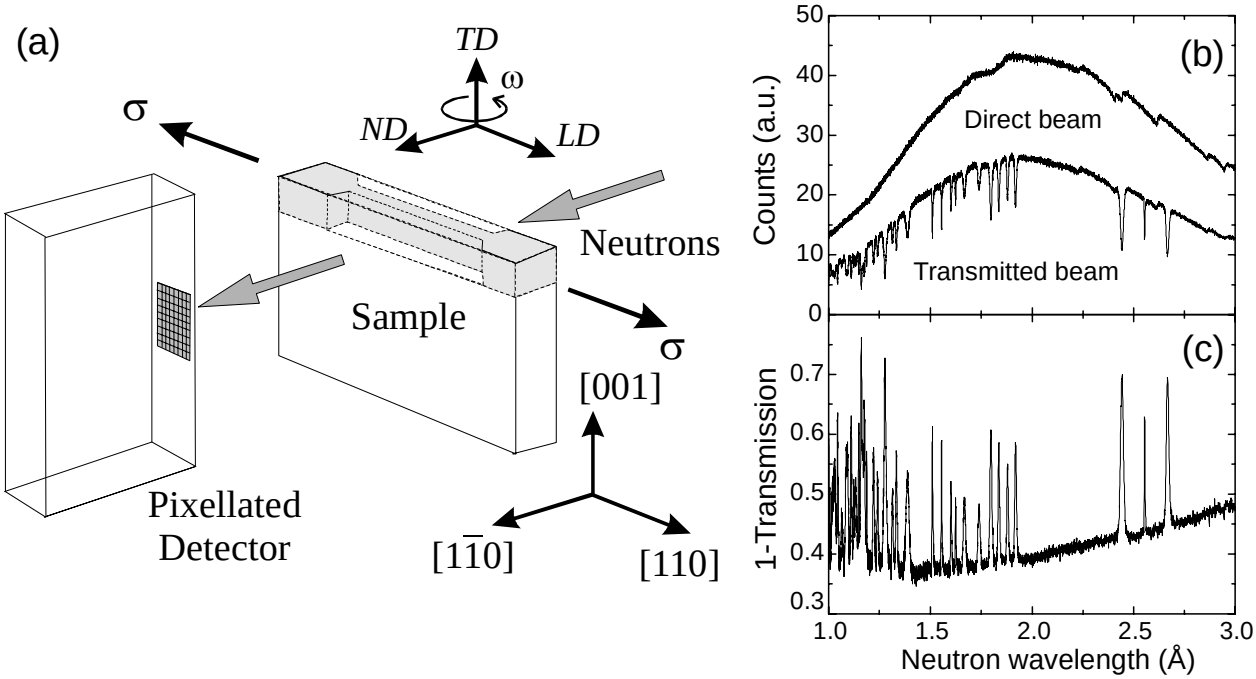

Fig. 1: (a) Experimental setup (b) Direct and transmitted neutron spectra (c) Normalized transmission. The peaks come from diffraction in crystal planes.

2. NEUTRON TRANSMISSION OF MOSAIC CRYSTALS

The transmission experiment is simple: the sample is placed in the neutron beam and a detector is located just behind the sample (Fig.1a). The transmission method essentially compares the reduction in intensity brought about by the insertion of a sample (Fig.1b). In a transmitted beam the neutrons that have interacted with the sample are missing. It is therefore possible to derive crystallographic information about the sample by analysing this transmitted spectrum. Neutron transmission experiments are performed at pulsed neutron sources where neutrons are produced in short pulses, so their wavelength is easily determined by their time of flight (TOF) along a fixed flight path. Moreover, by using a pixellated array of detectors that records the spatial variation of the transmission across the sample, it is possible to produce TOF "radiographies" in specimens having dimensions of centimetres. The experiments described here were performed on ENGIN-X, the beamline for engineering applications at the ISIS Facility,

UK. (Dann, Daymond, Edwards, James and Santisteban 2004). A pixellated transmission detector consisting of a 10x10 array of 2x2 mm ^{2} scintillation detectors was used, but the pixels were added up in columns for a faster count rate.

Dogbone specimens for the tensile tests were cut out by electro-discharge machining from a neutron monochromator (Fig.1a). The monochromator was a Cu mosaic crystal 100 mm long, 50 mm wide and 10 mm thick produced by hot pressing of a nearly-perfect Cu crystal (Frey 1974). Fig. 1c shows a typical transmission measured along the normal direction. The results are shown as *(1-Transmission)* for better clarity and to aid subsequent analysis. Our analysis exploits the sharp dips that appear in the transmitted intensity as a result of diffraction on the crystallographic planes. These dips (or peaks in 1-*Tr*) are just a different manifestation of the spots recorded in traditional Laue photographs. The position, width and intensity of these peaks are obtained by single-peak least-squares refinement. Results for a reduced number of peaks are listed in Table 1. The peak profiles are asymmetric and were described as the convolution of a Voigt function with a sharp-edged exponential decay.

2.1 Peak positions and crystal orientation. The positions of the diffraction peaks depend on the orientation between the incident beam and the crystal. From Bragg's law, it is easy to show that for a cubic crystal with lattice parameter a the hkl reflection will diffract neutrons of wavelength

$$\lambda_{hkl} = 2a\frac{\left|ha_{11} + ka_{12} + la_{13}\right|}{h^2 + k^2 + l^2}, \qquad (1)$$

where a_{11}, a_{12} and a_{13} are the direction cosines of the incident neutron beam in the coordinate system of the crystal. An alternative expression is

$$\lambda_{hkl} = 2d_{hkl}\cos\alpha_{hkl} \qquad (2)$$

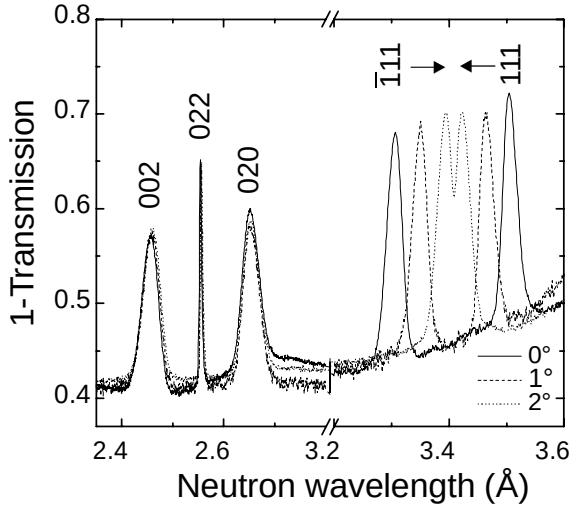

Fig.2: Peak shift induced by tilting .

where d_{hkl} is the distance between the planes perpendicular to the [hkl] direction and α_{hkl} is the angle between [hkl] and the neutron beam. So, after a reflection has been indexed, the angle between the incident beam and the normal to the diffraction planes can be precisely calculated. Hence, the dips appearing in the transmitted beam correspond to the projections of the interplanar distances d_{hkl} in the direction of the incident neutron beam. The peak positions can be exploited for a precise determination of the crystal orientation. This is easily achieved by a multi-linear regression of the observed peak positions λ_{hkl} using the direction cosines as independent variables (Eq. 1). The very good agreement between the experimental and calculated peak positions λ_{hkl} presented in Table 1 indicates the efficiency of this approach. The directions cosines give the coordinates of the incident neutron beam in the coordinate system of the crystal. In order to define the complete transformation matrix between the laboratory and crystal systems, we need to know the coordinates of at least two laboratory directions in the crystal system. So, we must record the transmission spectrum of the crystal at a second

orientation. Fig. 2 shows the dependence of the spectra on crystal orientation. It is clear that peaks shifts induced by a 1° rotation are easily resolved.

2.2 Peak widths and Mosaicity. The mosaicity of a crystal is characterized by recording rocking curves $W_{hkl}^{\boldsymbol{\tau}}(\phi)$. These rocking curves are a function of the rocking angle ϕ, the *hkl* reflection, and on the actual (diffraction) plane of the sample being investigated, identified here by the plane normal $\boldsymbol{\tau}$. The rocking curves measured using γ-rays reflect the intrinsic mosaicity of a specimen (Schneider 1974), whilst neutrons provides a convolution of the intrinsic mosaicity with the resolution of the instrument.The intrinsic mosaicity often has an irregular shape, but for practical purposes it is usually characterized by the full width at half maximum (FWHM) of $W_{hkl}^{\boldsymbol{\tau}}(\phi)$ (Sears 1997). The widths of the peaks in Fig. 2 vary strongly between reflections. The dependence of peak width on the experimental parameters is found by derivating Eq. (2)

Table 1. Typical peak parameters

	Position		Width	Angle
Refl.	Exp λ_{hkl} [Å]	Calc λ_{hkl} [Å]	$(\Delta\lambda_{hkl}/\lambda_{hkl})$ [X10^{-3}]	α_{hkl} [degrees]
2 0 0	3.3919 (1)	3.39252	3.2 (3)	20.17
1 $\bar{1}$ $\bar{1}$	3.2860 (1)	3.28774	5.8 (1)	38.04
1 1 $\bar{1}$	2.8298 (1)	2.82986	11.3 (1)	47.30
2 0 $\bar{2}$	2.29438 (5)	2.29410	3.3 (6)	26.11
3 $\bar{1}$ $\bar{1}$	2.13061 (5)	2.13030	1.8 (3)	12.09
3 1 $\bar{1}$	2.00508 (6)	2.00542	2.9 (3)	23.05
2 $\bar{2}$ 0	1.86815 (8)	1.86796	6.2 (2)	43.02

$$\left(\frac{\Delta\lambda_{hkl}}{\lambda_{hkl}}\right)^2 = \left(\frac{\Delta d_{hkl}}{d_{hkl}}\right)^2 + (\Delta\alpha_{hkl})^2 \tan^2\alpha_{hkl} + 2\left(\frac{\Delta d_{hkl}}{d_{hkl}}\right)\Delta\alpha_{hkl}\tan\alpha_{hkl} \qquad (3)$$

The first term $(\Delta d/d)^2$ corresponds to the broadening coming from deformation of the crystal lattice within the individual mosaic blocks, whereas the second term $(\Delta\alpha_{hkl})^2$ will come from a finite distribution of scattering angles, arising mainly from the misalignement of mosaic blocks, but also as a result of the divergence of the incident beam η. In most cases, the angular term is much larger that the broadening due to elastic deformation, so the peak width will be.

$$\left(\frac{\Delta\lambda_{hkl}}{\lambda_{hkl}}\right)^2 = \tan^2\alpha_{hkl}\left(\left\langle \mathrm{FWHM}^2\left(W_{hkl}^{\boldsymbol{\tau}}\right)\right\rangle + \left\langle\eta^2\right\rangle\right) \qquad (4)$$

This functional dependence of peak width on scattering angle has been corroborated in the present experiments. As changes in the scattering angle normal to the diffraction plane do not contribute to the observed peak broadening, the FWHM of the rocking curve $W_{hkl}^{\boldsymbol{\tau}}(\phi)$ can be readily extracted from the peaks measured in transmission.

3. TENSILE TESTS

We loaded the dogbone specimens along the [.697,.713,.061] longitudinal direction (LD) in strain control mode, followed by unloading in stress control mode (Fig. 3a) using ENGINX stress rig (Dann et al 2004). An elastic regime was found up to a stress load of 28 MPa, followed by yield and plastic deformation through slip in the (11-1)[101] and (11-1)[011] systems. The deformation mode was inferred by evaluation of Schmidt's

factors and by the change of the specimen's geometry. At each load, transmission spectra were recorded along two directions making angles of 62° and 63.3° with the loading axis. The seven peaks listed in Table 1 were analyzed in each case and the crystal orientation was calculated from their positions.

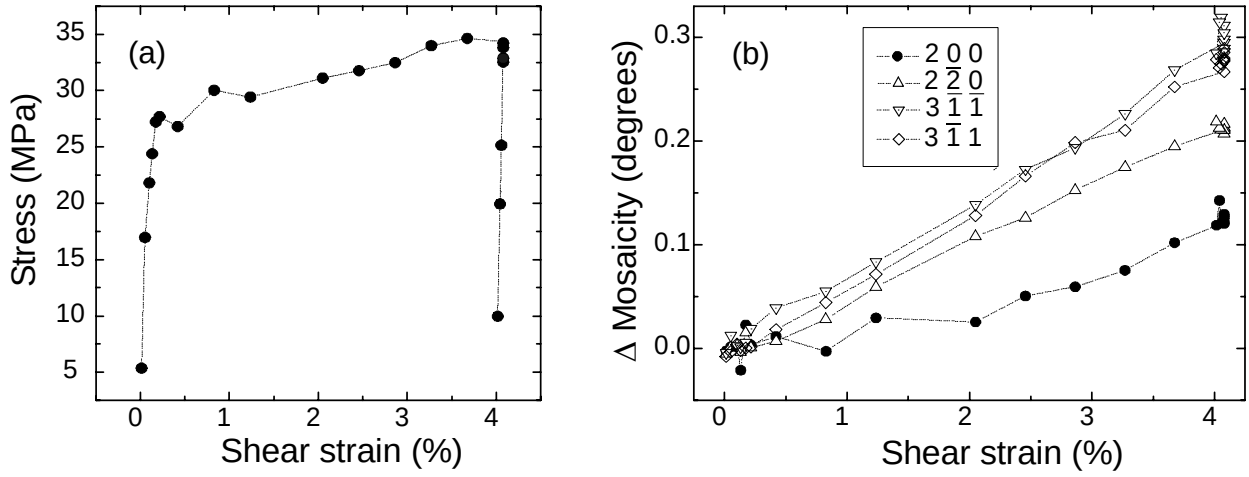

Fig. 3: (a) Strain-stress curve (b) Variation of mosaicity with deformation

3.1 Mosaicity. Fig. 3b shows the change in mosaicity registered for selected reflections. It is clear that the mosaicity increases as a result of plastic deformation, whilst it remains essentially constant through the elastic regime. The anisotropic evolution of the mosaic spread is also evident from the different slopes found for each reflection. For the [200] and [2-20] reflections the diffraction plane was nearly perpendicular to ND, whilst for [3-1-1] and [3-11] the diffraction plane was nearly perpendicular to LD.

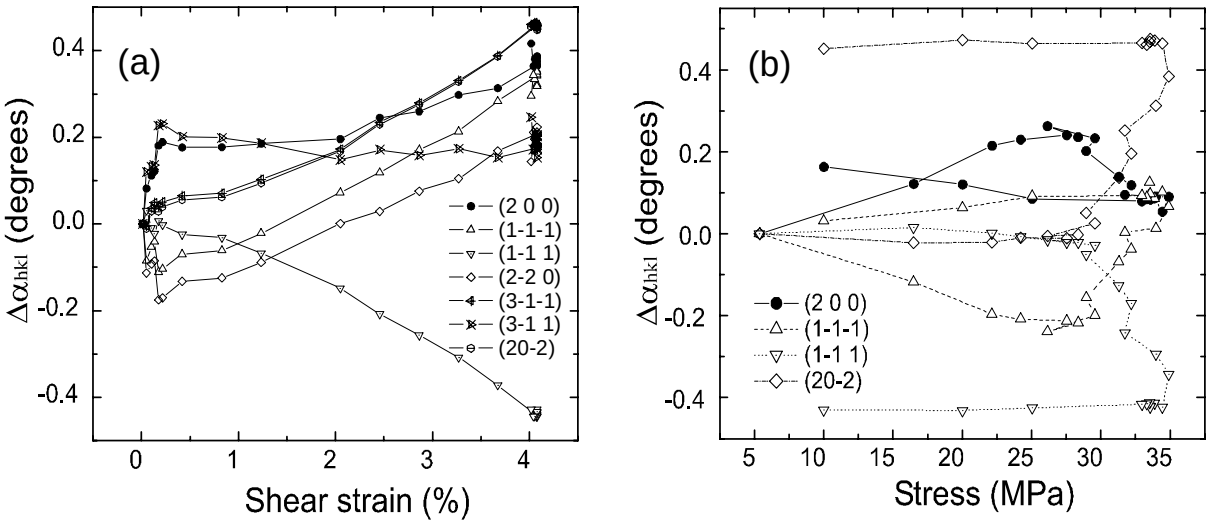

Fig. 4: Variation of the angle between [hkl] and the direction of tensile load (a) on strain (b) on applied stress

3.2 Crystal orientation. Fig.4a and 4b show the change in the angle that the [hkl] directions make with the loading axis as a function of applied strain and stress, respectively. The transition between the elastic and plastic regimes is also evident here, with most reflections showing an inflection point at the yield strain.

3.3 Spatial resolution.We also studied the variation of crystal orientation across the sample. Five spectra, corresponding to different sample positions along LD, were recorded for each orientation with the pixellated detector. The angular difference between the [100] directions measured at each position is shown in Fig. 5. A considerable misalignment is originally present in the sample. The external load tends to align the different parts of the specimen through the elastic regime, but this ceases after yielding.

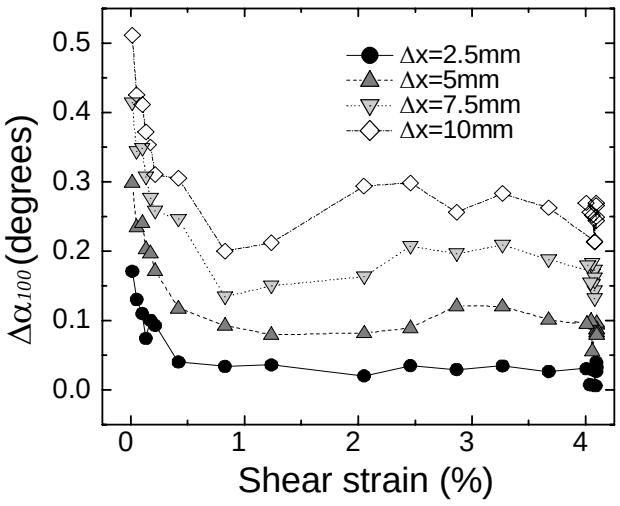

Fig. 5: Spatial variation of crystal orientation across the sample

3.4 Elastic strain The average difference Δ_{hkl} between experimental and calculated values is (Δ_{hkl} / λ_{hkl}) ~0003 or 300 με (1 με=10^{-6}). Although small, it is larger than the uncertainty in the peak position, neither presents a normal distribution when considered for all peaks. We believe this difference comes from elastic strains existing within the crystal lattice. It is possible to define the six components of the elastic strain tensor by considering a trigonal unit cell during the refinement of the crystal orientation However, such a model increases the number of parameters to be refined to nine, so a larger number of peaks would be needed in this case. Peak overlap sometimes prevents the application of the single peak refinement procedure used here, so a full pattern or Rietveld approach should be adopted for such goal.

4. CONCLUSIONS

Time-of-flight neutron transmission can be used to study the elastic and plastic deformation of mosaic crystals with spatial resolution. In its present state, the technique has a spatial resolution of 2x2 mm^2 and provides the mosaic spread and interplanar distances for several reflections simultaneously, as well as the mean orientation of the crystallites. The determination of the full elastic strain tensor through the incorporation of the lattice deformation in the analysis of the transmitted signal is the logical step forward.

REFERENCES

Dann, J.A., Daymond, M.R., Edwards, L., James, J., and Santisteban, J.R. (2004). ENGIN-X: A New Diffractometer Optimised for Stress Measurement. Physica B (In press)

Frey, F. (1974). A neutron monochromator system consisting of deformed crystals with anisotropic mosaic structure. Nucl. Instr. Meth. 124, 93-99.

Schneider, J.R. (1974). A γ-ray diffractometer: a tool for investigating mosaic structure. J. Appl. Cryst. 7, 541-546.

Sears, V.F (1997). Bragg reflection in mosaic Crystals. Acta Cryst. A53, 35-54.